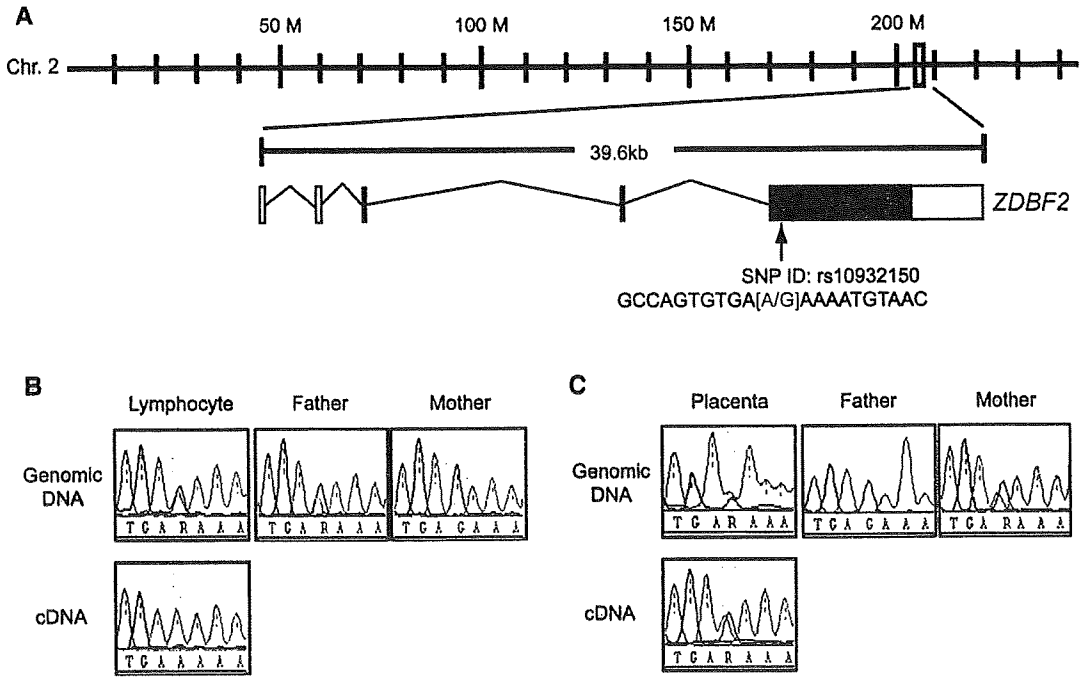

Fig. 6. Expression analysis of the *ZDBF2* gene on human chromosome 2. (A) Genomic structure of the human *ZDBF2* gene. The arrow indicates the position of the SNP (ID: rs10932150). The SNP sequence is indicated in red. Allele-specific RT-PCR sequencing analysis in (B) the human lymphocyte cell line and (C) placenta. The SNP of exon 5 is highlighted in yellow.

adult CD-1 mouse uterus. The 9.5-, 15.5-, and 18.5-day-old embryos were harvested, and TRIzol (Invitrogen, Carlsbad, CA) was used to extract total RNA from the embryos.

cRNA preparation and microarray hybridization

A 1-μg aliquot of total RNA was used as the template for cDNA synthesis (Eukaryotic Poly-A RNA Control Kit and One-Cycle cDNA Synthesis Kit; Affymetrix, Santa Clara, CA). The cDNA was purified with the Sample Cleanup Module (Affymetrix). Following cleanup, biotin-labeled cRNA was synthesized using the GeneChip IVT Labeling Kit (Affymetrix), and fragmented and purified with the Sample Cleanup Module (Affymetrix). The fragmented cRNA was hybridized with Affymetrix Mouse genome 430 2.0 GeneChip at 45 °C for 16 h. The GeneChips were then washed and stained with a GeneChip Fluidics Station 460 (Affymetrix) according to the Expression Analysis Technical Manual. An Affymetrix GeneChip Scanner 3000 was used to quantify the signal.

Microarray data analyses

The Affymetrix Mouse genome 430 2.0 GeneChip contains 45101 genes and ESTs. We compared the parthenogenetic embryos with control embryos by using the following 3 normalization methods: data transformation, where the set measurements were less than 0.01–0.01; per chip normalization, where the values were normalized to the 50th percentile to limit the range of variation; and per gene normalization, where the values were normalized to specific samples.

Polymorphism analyses among candidate genes

C57BL/6 and DBA/2 mice were purchased from Clea Japan, and JF1 mice [53] obtained from the National Institute of Genetics in Mishima, Japan. Genomic DNA was isolated from the tails of C57BL/6, DBA/2, and JF1 mice by digestion with proteinase K (Invitrogen), which was followed by phenol/chloroform extraction. The DNA was amplified by PCR with TaKaRa *Ex Taq* polymerase (TaKaRa, Kyoto, Japan). The primer sequences were complementary to the exon sequences of the candidate genes, and the PCR conditions are listed in Supplemental Table 1. The PCR products were purified with Wizard SV Gel and the PCR Clean-Up System (Promega, Madison, WI). PCR amplification was performed with TaKaRa *Ex Taq* polymerase. The purified PCR products were sequenced with primers for the direct sequence and the ABI PRISM 3130 Genetic Analyzer (Applied Biosystems, Foster, CA).

RT-PCR and allelic expression analyses among candidate genes

Using TRIzol (Invitrogen), we isolated total RNA from BDF1, DBF1 (DBA/2×C57BL/6), JBF1 (JF1×C57BL/6), and BJF1 (C57BL/6×JF1) embryos at day 9.5. After total RNA was treated with DNase (Promega) to exclude the genomic DNA, the absence of genomic DNA contamination was confirmed by the lack of amplification of GAPDH by PCR. The genomic DNA-free total RNA was reverse transcribed to cDNA with SuperScript II (Invitrogen). The expression of 22 candidate imprinted genes was examined by RT-PCR. The primer sequences and PCR conditions are listed in Supplemental Table 1 and Supplemental Table 2. To investigate the expression patterns of *Zdbf2*, different tissues at various developmental stages (15.5-, and 18.5-day-old embryos and 1- and 9-week-old mice) were harvested, and TRIzol (Invitrogen, Carlsbad, CA) was used to extract total RNA.

5′-RACE analysis

The 5′-region of the mouse *Zdbf2* gene was obtained using the 5′-Full RACE Core Set (TaKaRa). Total RNA was prepared from 9.5-day-old BJF1 embryos, and a *Zdbf2* gene-specific 5′-end phosphorylated primer (P2, 5′-ATTCCAAGGACTGCTGCTGT-3′) was used. We performed 2 rounds of PCR by using TaKaRa *LA Taq* (TaKaRa) under the following conditions: 25 cycles of 30 s at 94 °C, 30 s at 55 °C, and 4 min at 72 °C for the first PCR and 25 cycles of 30 s at 94 °C, 30 s at 60 °C, and 4 min at 72 °C for the second PCR. The primer sets

used for the nested PCR were as follows: Sense S1, 5′-TAGACCTGG-TACTTCTCAGGAACA-3′ and anti-sense A1, 5′-CAACAGATCCTGAATCC-TCGGAGT-3′ for the first PCR; sense S2, 5′-CACGCAGAAGTTGCAGTTCG-3′ and anti-sense A2, 5′-TCTGCACCGCTATCTGCAG-3′ for the second PCR. The amplified products were purified and directly sequenced.

DNA methylation analyses

Genomic DNA samples isolated from 9.5-day-old parthenogenetic, androgenetic, and control embryos or from the sperm and oocytes of adult BJF1 mice were treated with sodium bisulfite [26] using the EpiTect Bisulfite Kit (QIAGEN, Valencia, CA). The bisulfite-treated DNA was amplified by PCR with TaKaRa *Ex Taq* Hot Start Version (TaKaRa) for CpG-rich regions around the mouse *Zdbf2* gene. The primers and PCR conditions for the amplification are listed in Supplemental Table 3. The PCR products were subcloned into pGEM-T Easy vector (Promega), which was transformed into DH5α cells. Colonies were selected and transferred into 96-well plates, and DNA was amplified by rolling circle amplification [54] with an Illustra TempliPhi DNA amplification kit (GE Healthcare Bio-Sciences, Little Chalfont, UK). DNA was sequenced using standard primers (SP6, 5′-GATTTAGGTGA-CACTATAG-3′ and T7, 5′-TAATACGACTCACTATAGGG-3′) and the ABI PRISM 3130 Genetic Analyzer (Applied Biosystems). The percentage of methylation was calculated as the number of methylated CpG dinucleotides from the total number of CpGs at every CpG island (CpG-rich region). At least 5 clones from each region and each parental allele were sequenced.

Expression analysis of human ZDBF2

This study was approved by the Institutional Review Board Committee at National Center for Child Health and Development, and performed after obtaining written informed consent from each subject or his or her parent(s). Genomic DNA was isolated from human lymphocytes with the use of a FlexiGene DNA Kit (Qiagen). Total RNA was extracted from human lymphocyte cell lines with RNeasy Plus Mini Kit (Qiagen), and the total RNA from human placenta was extracted with ISOGEN (Nippon Gene, Tokyo, Japan). The extracted RNA was DNase-treated with deoxyribonuclease (RT Grade) for heat stop (Nippon Gene). DNase-treated RNA was purified by phenol/chloroform extraction. The genomic DNA-free total RNA was reverse transcribed to cDNA with SuperScript III (Invitrogen). PCR carried out in a 50-μl volume reaction mixture containing cDNA (equivalent of 20–50 ng total RNA), 1× PCR buffer, 2.5 U of AmpliTaq Gold (Applied Biosystems), 50 pmol of each primer, and 10 mM dNTPs. The primers used for human *ZDBF2* were 5′-AAACTGGA-GAAGGGACAGCA-3′ and 5′-CAAATGAGCTGCTGGTGGTA-3′. The cycling protocol was as follows: 1 min at 94 °C; 30 cycles of 94 °C for 1 min, 57 °C for 1 min, and 72 °C for 1 min; and 5 min at 72 °C.

Acknowledgments

We thank Hiroyuki Sasaki for helpful discussions. This work was supported by Grants-in-Aid for Scientific Research on Priority Area, and for Scientific Research A from the Ministry of Education, Science, Culture and Sports of Japan to T.K.

Appendix A. Supplementary data

Supplementary data associated with this article can be found, in the online version, at doi:10.1016/j.ygeno.2008.12.012.

References

[1] W. Reik, J. Walter, Genomic imprinting: parental influence on the genome, Nat. Rev. Genet. 2 (2001) 21–32.
[2] E. Li, T.H. Bestor, R. Jaenisch, Targeted mutation of the DNA methyltransferase gene results in embryonic lethality, Cell 69 (1992) 915–926.
[3] D. Bourc'his, G.L. Xu, C.S. Lin, B. Bollman, T.H. Bestor, Dnmt3L and the establishment of maternal genomic imprints, Science 294 (2001) 2536–2539.
[4] K. Hata, M. Okano, H. Lei, E. Li, Dnmt3L cooperates with the Dnmt3 family of de novo DNA methyltransferases to establish maternal imprints in mice, Development 129 (2002) 1983–1993.
[5] M. Kaneda, et al., Essential role for de novo DNA methyltransferase Dnmt3a in paternal and maternal imprinting, Nature 429 (2004) 900–903.
[6] E. Li, C. Beard, R. Jaenisch, Role for DNA methylation in genomic imprinting, Nature 366 (1993) 362–365.
[7] R. Hirasawa, et al., Maternal and zygotic Dnmt1 are necessary and sufficient for the maintenance of DNA methylation imprints during preimplantation development, Genes Dev. 22 (2008) 1607–1616.
[8] L.D. Hurst, G. McVean, T. Moore, Imprinted genes have few and small introns, Nat. Genet. 12 (1996) 234–237.
[9] J.M. Greally, Short interspersed transposable elements (SINEs) are excluded from imprinted regions in the human genome, Proc. Natl. Acad. Sci. U. S. A. 99 (2002) 327–332.
[10] X. Ke, N.S. Thomas, D.O. Robinson, A. Collins, The distinguishing sequence characteristics of mouse imprinted genes, Mamm. Genome 13 (2002) 639–645.
[11] B. Neumann, P. Kubicka, D.P. Barlow, Characteristics of imprinted genes, Nat. Genet. 9 (1995) 12–13.
[12] H. Kobayashi, et al., Bisulfite sequencing and dinucleotide content analysis of 15 imprinted mouse differentially methylated regions (DMRs): paternally methylated DMRs contain less CpGs than maternally methylated DMRs, Cytogenet. Genome Res. 113 (2006) 130–137.
[13] D. Jia, R.Z. Jurkowska, X. Zhang, A. Jeltsch, X. Cheng, Structure of Dnmt3a bound to Dnmt3L suggests a model for de novo DNA methylation, Nature 449 (2007) 248–251.
[14] Y. Hayashizaki, et al., Identification of an imprinted U2af binding protein related sequence on mouse chromosome 11 using the RLGS method, Nat. Genet. 6 (1994) 33–40.
[15] C. Plass, et al., Identification of Grf1 on mouse chromosome 9 as an imprinted gene by RLGS-M, Nat. Genet. 14 (1996) 106–109.
[16] T. Kaneko-Ishino, et al., Peg1/Mest imprinted gene on chromosome 6 identified by cDNA subtraction hybridization, Nat. Genet. 11 (1995) 52–59.
[17] Y. Kuroiwa, et al., Peg3 imprinted gene on proximal chromosome 7 encodes for a zinc finger protein, Nat. Genet. 12 (1996) 186–190.
[18] N. Miyoshi, et al., Identification of the Meg1/Grb10 imprinted gene on mouse proximal chromosome 11, a candidate for the Silver–Russell syndrome gene, Proc. Natl. Acad. Sci. U. S. A. 95 (1998) 1102–1107.
[19] N. Miyoshi, et al., Identification of an imprinted gene, Meg3/Gtl2 and its human homologue MEG3, first mapped on mouse distal chromosome 12 and human chromosome 14q, Genes Cells 5 (2000) 211–220.
[20] Y. Hagiwara, et al., Screening for imprinted genes by allelic message display: identification of a paternally expressed gene impact on mouse chromosome 18, Proc. Natl. Acad. Sci. U. S. A. 94 (1997) 9249–9254.
[21] S. Kobayashi, et al., Mouse Peg9/Dlk1 and human PEG9/DLK1 are paternally expressed imprinted genes closely located to the maternally expressed imprinted genes: mouse Meg3/Gtl2 and human MEG3, Genes Cells 5 (2000) 1029–1037.
[22] Y. Mizuno, et al., Asb4, Ata3, and Dcn are novel imprinted genes identified by high-throughput screening using RIKEN cDNA microarray, Biochem. Biophys. Res. Commun. 290 (2002) 1499–1505.
[23] R. Schulz, et al., Chromosome-wide identification of novel imprinted genes using microarrays and uniparental disomies, Nucleic. Acids Res. 34 (2006) e88.
[24] A.J. Wood, et al., A screen for retrotransposed imprinted genes reveals an association between X chromosome homology and maternal germ-line methylation, PLoS Genet. 3 (2007) e20.
[25] P.P. Luedi, A.J. Hartemink, R.L. Jirtle, Genome-wide prediction of imprinted murine genes, Genome Res. 15 (2005) 875–884.
[26] M. Frommer, et al., A genomic sequencing protocol that yields a positive display of 5-methylcytosine residues in individual DNA strands, Proc. Natl. Acad. Sci. U. S. A. 89 (1992) 1827–1831.
[27] A.C. Ferguson-Smith, H. Sasaki, B.M. Cattanach, M.A. Surani, Parental-origin-specific epigenetic modification of the mouse H19 gene, Nature 362 (1993) 751–755.
[28] H. Shibata, et al., A methylation imprint mark in the mouse imprinted gene Grf1/Cdc25Mm locus shares a common feature with the U2afbp-rs gene: an association with a short tandem repeat and a hypermethylated region, Genomics 49 (1998) 30–37.
[29] S. Takada, et al., Epigenetic analysis of the Dlk1-Gtl2 imprinted domain on mouse chromosome 12: implications for imprinting control from comparison with Igf2-H19, Hum. Mol. Genet. 11 (2002) 77–86.
[30] V.M. Kalscheuer, E.C. Mariman, M.T. Schepens, H. Rehder, H.H. Ropers, The insulin-like growth factor type-2 receptor gene is imprinted in the mouse but not in humans, Nat. Genet. 5 (1993) 74–78.
[31] K. Okamura, et al., Comparative genome analysis of the mouse imprinted gene impact and its nonimprinted human homolog IMPACT: toward the structural basis for species-specific imprinting, Genome Res. 10 (2000) 1878–1889.
[32] U. Spiekerkoetter, et al., Uniparental disomy of chromosome 2 resulting in lethal trifunctional protein deficiency due to homozygous alpha-subunit mutations, Hum. Mutat. 20 (2002) 447–451.
[33] D.A. Thompson, et al., Retinal dystrophy due to paternal isodisomy for chromosome 1 or chromosome 2, with homoallelism for mutations in RPE65 or MERTK, respectively, Am. J. Hum. Genet. 70 (2002) 224–229.
[34] B. Chavez, E. Valdez, F. Vilchis, Uniparental disomy in steroid 5alpha-reductase 2 deficiency, J. Clin. Endocrinol. Metab. 85 (2000) 3147–3150.

[35] F.M. Petit, et al., Paternal isodisomy for chromosome 2 as the cause of Crigler–Najjar type I syndrome, Eur. J. Hum. Genet. 13 (2005) 278–282.
[36] R.J. Smith, W. Dean, G. Konfortova, G. Kelsey, Identification of novel imprinted genes in a genome-wide screen for maternal methylation, Genome Res. 13 (2003) 558–569.
[37] G. Piras, et al., Zac1 (Lot1), a potential tumor suppressor gene, and the gene for epsilon-sarcoglycan are maternally imprinted genes: identification by a subtractive screen of novel uniparental fibroblast lines, Mol. Cell. Biol. 20 (2000) 3308–3315.
[38] M.P. Lee, et al., Loss of imprinting of a paternally expressed transcript, with antisense orientation to KVLQT1, occurs frequently in Beckwith–Wiedemann syndrome and is independent of insulin-like growth factor II imprinting, Proc. Natl. Acad. Sci. U. S. A. 96 (1999) 5203–5208.
[39] J. Peters, et al., A cluster of oppositely imprinted transcripts at the Gnas locus in the distal imprinting region of mouse chromosome 2, Proc. Natl. Acad. Sci. U. S. A. 96 (1999) 3830–3835.
[40] N. Ruf, et al., Expression profiling of uniparental mouse embryos is inefficient in identifying novel imprinted genes, Genomics 87 (2006) 509–519.
[41] R. Kikuno, et al., HUGE: a database for human KIAA proteins, a 2004 update integrating HUGEppi and ROUGE, Nucleic. Acids Res. 32 (2004) D502–D504.
[42] F. Guillemot, A. Nagy, A. Auerbach, J. Rossant, A.L. Joyner, Essential role of Mash-2 in extraembryonic development, Nature 371 (1994) 333–336.
[43] T. Kono, et al., Birth of parthenogenetic mice that can develop to adulthood, Nature 428 (2004) 860–864.
[44] M. Kawahara, et al., High-frequency generation of viable mice from engineered bimaternal embryos, Nat. Biotechnol. 25 (2007) 1045–1050.
[45] T.L. Davis, J.M. Trasler, S.B. Moss, G.J. Yang, M.S. Bartolomei, Acquisition of the H19 methylation imprint occurs differentially on the parental alleles during spermatogenesis, Genomics 58 (1999) 18–28.
[46] T. Ueda, et al., The paternal methylation imprint of the mouse H19 locus is acquired in the gonocyte stage during foetal testis development, Genes Cells 5 (2000) 649–659.
[47] J.Y. Li, D.J. Lees-Murdock, G.L. Xu, C.P. Walsh, Timing of establishment of paternal methylation imprints in the mouse, Genomics 84 (2004) 952–960.
[48] H. Hiura, et al., DNA methylation imprints on the IG-DMR of the Dlk1–Gtl2 domain in mouse male germline, FEBS Lett. 581 (2007) 1255–1260.
[49] Y. Kato, et al., Role of the Dnmt3 family in de novo methylation of imprinted and repetitive sequences during male germ cell development in the mouse, Hum. Mol. Genet. 16 (2007) 2272–2280.
[50] B.J. Yoon, et al., Regulation of DNA methylation of Rasgrf1, Nat. Genet. 30 (2002) 92–96.
[51] A. Lewis, K. Mitsuya, M. Constancia, W. Reik, Tandem repeat hypothesis in imprinting: deletion of a conserved direct repeat element upstream of H19 has no effect on imprinting in the Igf2-H19 region, Mol. Cell. Biol. 24 (2004) 5650–5656.
[52] Y. Obata, et al., Post-implantation development of mouse androgenetic embryos produced by in-vitro fertilization of enucleated oocytes, Hum. Reprod. 15 (2000) 874–880.
[53] T. Koide, et al., A new inbred strain JF1 established from Japanese fancy mouse carrying the classic piebald allele, Mamm. Genome 9 (1998) 15–19.
[54] J.R. Nelson, et al., TempliPhi, phi29 DNA polymerase based rolling circle amplification of templates for DNA sequencing, Biotechniques Suppl. (2002) 44–47.

Maternal Uniparental Disomy 14 Syndrome Demonstrates Prader-Willi Syndrome-Like Phenotype

Kana Hosoki, MS, Masayo Kagami, MD, PhD, Touju Tanaka, MD, PhD, Masaya Kubota, MD, PhD, Kenji Kurosawa, MD, PhD, Mitsuhiro Kato, MD, PhD, Kimiaki Uetake, MD, Jun Tohyama, MD, PhD, Tsutomu Ogata, MD, PhD, and Shinji Saitoh, MD, PhD

Objective To delineate the significance of maternal uniparental disomy 14 (upd(14)mat) and related disorders in patients with a Prader-Willi syndrome (PWS)–like phenotype.
Study design We examined 78 patients with PWS-like phenotype who lacked molecular defects for PWS. The *MEG3* methylation test followed by microsatellite polymorphism analysis of chromosome 14 was performed to detect upd(14)mat or other related abnormalities affecting the 14q32.2-imprinted region.
Results We identified 4 patients with upd(14)mat and 1 patient with an epimutation in the 14q32.2 imprinted region. Of the 4 patients with upd(14)mat, 3 had full upd(14)mat and 1 was mosaic.
Conclusions Upd(14)mat and epimutation of 14q32.2 represent clinically discernible phenotypes and should be designated "upd(14)mat syndrome." This syndrome demonstrates a PWS-like phenotype particularly during infancy. The *MEG3* methylation test can detect upd(14)mat syndrome defects and should therefore be performed for all undiagnosed infants with hypotonia. *(J Pediatr 2009;155:900-3)*.

Maternal uniparental disomy 14 (upd(14)mat) is characterized by prenatal and postnatal growth retardation, neonatal hypotonia, small hands and feet, feeding difficulty, and precocious puberty.[1] Chromosome 14q32.2 contains several imprinted genes, and loss of expression of paternally expressed genes including *DLK1* and *RTL1* is believed to be responsible for upd(14)mat phenotype.[2] Thus far, 5 patients with epimutations and 4 patients with a microdeletion affecting the 14q32.2 imprinted region have been reported to have upd(14)mat-like phenotype.[2-4] Paternal uniparental disomy 14 (upd(14)pat) shows a distinct and much more severe phenotype characterized by facial abnormality, bell-shaped thorax and abdominal wall defects.[1] Initially, upd(14)mat was identified in patients with Robertsonian translocations involving chromosome 14, but increasing numbers of patients with a normal karyotype have been recognized.[1,5] Because maternal uniparental disomy 15 is responsible for the condition in more than 20% of patients with Prader-Willi syndrome (PWS), of which the overall prevalence is more than 1 in 15000 births,[6] one could suspect that upd(14)mat is underestimated. Phenotype of upd(14)mat is known to resemble that of PWS, which is characterized by neonatal hypotonia, small hands and feet, mental retardation, and hyperphagia resulting in obesity beyond infancy. Mitter et al[7] recently reported that upd(14)mat was detected in 4 of 33 patients who were suspected to have PWS and raised the question that upd(14)mat could be present in patients with PWS-like phenotype. Thus we examined patients who presented with PWS-like phenotype, but in whom PWS had been excluded.

Methods

The median age of the 78 patients enrolled in the study was 18.5 months, and the range was 1.4 to 324 months. Sex ratio was 1:1. All patients demonstrated PWS-like phenotype including hypotonia during infancy. We initially performed the *SNURF-SNRPN* DNA methylation test, and normal methylation results excluded the diagnosis of PWS.[8]

This study was approved by the Institutional Review Board Committees at Hokkaido University Graduate School of Medicine and National Center for Child Health and Development. The parents of the patients gave written informed consent.

DNA methylation status at the promoter region of imprinted *MEG3*, located in 14q32.2, was examined (**Figure 1**). Genomic DNA was extracted from leukocytes and treated with sodium bisulfite, and methylated allele– and unmethylated allele–specific primers were used to polymerase chain reaction amplify each allele, as described previously.[9] If aberrant DNA methylation was identified,

PWS	Prader-Willi syndrome
Upd(14)mat	Maternal uniparental disomy 14
Upd(14)pat	Paternal uniparental disomy 14

From the Department of Pediatrics, Hokkaido University Graduate School of Medicine, Sapporo (K.H., S.S.), the Department of Endocrinology and Metabolism (M.Kagami, T.O.), the Division of Clinical Genetics and Molecular Medicine (T.T.), and the Department of Pediatric Neurology (M. Kubota), National Research Institute for Child Health and Development, Tokyo, the Division of Medical Genetics, Kanagawa Children's Medical Center, Yokohama (K.K.), the Department of Pediatrics, Yamagata University School of Medicine, Yamagata (M. Kato), the Department of Pediatrics, Obihiro Kosei Hospital, Obihiro (K.U.), and the Department of Pediatrics, Nishi-Niigata Chuo National Hospital, Niigata (J.T.), Japan

This work was partially supported by a grant from the Ministry of Education, Science and Culture of Japan. The authors declare no conflicts of interest.

 10.1016/j.jpeds.2009.06.045

we carried out microsatellite polymorphism analysis for 16 loci on chromosome 14 (ABI PRISM Linkage Mapping Set v2.5; Applied Biosystems, Foster City, California) with DNA from the patients and their parents (**Figure 1**). Polymerase chain reaction products were analyzed on an ABI310 automatic capillary genetic analyzer and with GeneMapper software (Applied Biosystems). If aberrant DNA methylation was identified but the patient demonstrated biparental origin of the chromosome 14s, we further examined the chromosomes for DNA methylation state, parental origin, and microdeletion in 14q32.2, as described previously.[2, 3]

Results

We identified abnormal hypomethylation at the *MEG3* promoter in 5 of 78 patients (**Figure 2**). Almost complete lack of methylation was found in 4 patients (case 1 to 4), but 1 patient (case 5) demonstrated faint methylation. Polymorphism studies demonstrated that 3 (cases 2 to 4) of the 4 patients with complete lack of *MEG3* promoter methylation had complete upd(14)mat, but 1 patient (case 1) had inherited both parental alleles (**Table I**; available at www.jpeds.com). We further examined the DNA methylation state and microdeletion or segmental upd at 14q32.3, and concluded that this patient (case 1) had an epimutation. The detailed data have been reported previously.[3] The patient (case 5) with faint *MEG3* methylation was demonstrated to have 2 maternal alleles, as well as 1 paternal allele with lower signal intensity. This indicated mosaicism of upd(14)mat (80%) and a normal karyotype (20%) (**Figure 3**; available at www.jpeds.com).

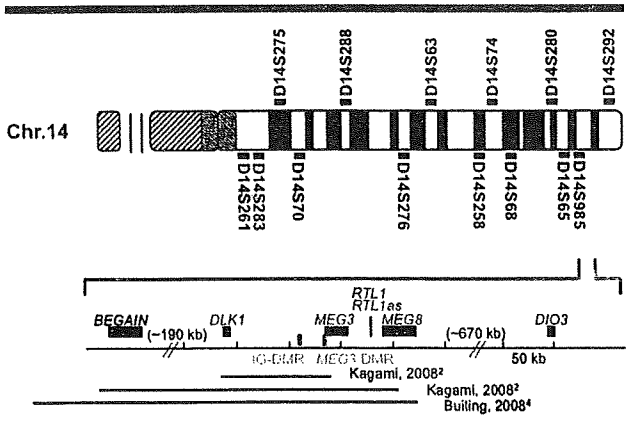

Figure 1. Schematic map of the 14q32.2 imprinted region. Loci on chromosome 14 represent markers used for microsatellite polymorphism analysis. Paternally expressed genes are shown in *blue*, maternally expressed genes in *red*, and nonimprinted genes are shown in *black*. Differentially methylated regions (DMRs) are shown in *green*. *IG-DMR*, Intergenic DMR. Reported microdeletions are demonstrated as *horizontal bars*.

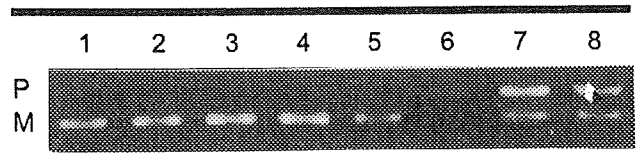

Figure 2. *MEG3* methylation test. *P*, Paternal methylated signal; *M*, maternal unmethylated signal; *1-5*, cases 1-5, respectively; *6*, paternal uniparental disomy 14; *7*, patient with PWS; *8*, normal control. Cases 1-4 show only the maternal unmethylated signal, and case 5 shows a faint paternal methylated signal.

The profiles of the patients with upd(14)mat or an epimutation are shown in **Table II**. We compared clinical features in these patients (**Table III**). All patients were referred to us during infancy because of hypotonia and motor developmental delay. Small hands and feet were also present in all patients. Prenatal growth retardation was present in all but 1 patient (case 1) who was later shown to have an epimutation. However, this patient had development of postnatal growth retardation, which was present in all patients. Premature onset of puberty was not evaluated in this study because the patients were too young. Apparent intellectual delay was only present in the patient who had upd(14)mat mosaicism (case 5). The clinical features of the patients with epimutation or with mosaic upd(14)mat were not distinct from those of the patients with full upd(14)mat.

Discussion

We detected 5 patients with upd(14)mat or epimutation at the 14q32.2-imprinted region in 78 subjects who had initially been suspected to have PWS. Mitter et al[7] reported that upd(14)mat was detected in 4 of 33 patients who were suspected to have PWS. However, Cox et al[10] reported that they did not find any upd(14)mat in 35 patients suspected to have PWS. Our study suggests that a significant number of patients with upd(14)mat are suspected to have PWS during infancy. To clarify how upd(14)mat and PWS share clinical features, we examined the clinical manifestations of our patients with upd(14)mat or an epimutation. All patients showed neonatal hypotonia and were referred to us during infancy. Feeding difficulty in the neonatal period and small hands and feet were also common to these patients and resembled features of PWS. It is noteworthy that all patients were referred during infancy, suggesting that upd(14)mat and PWS resemble each other, particularly during this period. Therefore upd(14)mat and related disorders, as well as PWS, should be important differential diagnoses for infants with hypotonia and feeding difficulty. Distinct features for upd(14)mat included less-specific facial characteristics, constant prenatal growth failure, and better intellectual development. Precocious puberty is not present in PWS; however, this was not evaluated in this study because the patients were not

Table II. Profiles of the patients with upd(14)mat and epimutation of 14q32.2

	Case 1	Case 2	Case 3	Case 4	Case 5
Molecular class	Epimutation	Upd(14)mat	Upd(14)mat	Upd(14)mat	Upd(14)mat (mosaic)
Age	2 y 2 m	4 y 2 m	2 y 7 m	1 y 9 m	3 y 4 m
Sex	Female	Male	Female	Female	Female
Karyotype	46,XX	46,XY	46,XX	46,XX	46,XX
Gestational age	41 w 5d	36 w 1 d	37 w 3 d	40 w 4 d	36 w
Birth weight g (SD)	3034 (0)	1955 (−2.6)	1680 (−3.3)	1858 (−2.8)	1434 (−3.9)
Birth length cm (SD)	50 (+0.7)	45.7 (−1.5)	40 (−4.0)	45 (−1.6)	39 (−3.9)
Birth OFC cm (SD)	Unknown	32 (−1.0)	30.4 (−2.0)	32 (−0.8)	30 (−2.2)
Present height cm (SD)	76.1 (−3.1)	89.5 (−2.8)	79 (−2.7)	72.5 (−3.4)	77.8 (−4.5)
Present weight kg (SD)	8.18 (−2.4)	11.6 (−2.1)	8.4 (−2.8)	6.4 (−3.7)	8.84 (−3.3)
Present OFC cm (SD)	45.2 (−1.5)	51.0 (+0.5)	48 (0)	44 (−1.8)	46.0 (−1.6)

old enough to demonstrate this feature. It is possible that when the patients get older, the clinical features of upd(14)mat may become more distinct from those of PWS.

We detected an epimutation in the 14q32.2-imprinted region, as well as upd(14)mat. The clinical features of the patient with the epimutation were grossly similar to those of patients with upd(14)mat. Thus far 5 patients with an epimutation in the paternal allele, including our patient, have been identified.[4,11] These patients exhibit clinical features indistinguishable from those with full upd(14)mat. Our patient with an epimutation demonstrated normal birth weight, but previously reported patients with an epimutation have shown intrauterine growth retardation. [4,11] Therefore normal birth weight is not a specific feature related to epimutation.

One of the patients with upd(14)mat was mosaic for upd(14)mat and normal karyotype. It is not easy to understand the pathogenesis of such a mosaic, but similar mosaicism of chromosome 15 has been reported.[12] Mosaicism for upd(15)mat and normal cell lines has been found in a patient with the PWS phenotype.[12] Similarly, our patient with mosaic upd(14)mat demonstrated typical clinical features of upd(14)mat. This could be explained by the small proportion of normal cell lines (less than 20%), or it could be that the level of mosaicism is different in each tissue. It is possible that the proportion of normal cells may be lower in the brain, which is most responsible for the phenotype of upd(14)mat.

As is clear in our series of patients, upd(14)mat phenotype can be caused by an epimutation of 14q32.2. Recently, Kagami et al[2] reported a microdeletion in 14q32.2 associated with a similar phenotype (**Figure 1**). Buiting et al[4] also reported a patient with a 1Mb deletion at 14q32.2 (**Figure 1**). Therefore upd(14)mat phenotype is associated with not only upd(14)mat but an epimutation or small deletion. This genetic complexity is similar to that of PWS. PWS is caused by paternal deletion of 15q11-q13, maternal uniparental disomy of chromosome 15, and epimutation (imprinting defect). A new name such as upd(14)mat syndrome would be appropriate to represent the entire upd(14)mat clinical features represented by upd(14)mat, epimutation of 14q32.2 and microdeletion in 14q32.2. Alternatively, Buiting et al[4] suggested the term, "Temple syndrome," because upd(14)mat was first described by Dr. I. K. Temple in 1991, who subsequently described an epimutation in 2007.[4,5,11]

Finally, it should be emphasized that the *MEG3* methylation test could detect not only upd(14)mat but an epimutation and small deletions involving *MEG3*.This is because the *MEG3* DMR that is used for the diagnostic DNA methylation test is involved in the shortest region of overlap of the microdeletions (**Figure 1**). It is therefore a powerful method for screening patients with upd(14)mat syndrome.

Table III. Clinical features in patients with upd(14)mat, epimutation and microdeletions of 14q32.2

	Present study					Previous studies		
	Case 1	Case 2	Case 3	Case 4	Case 5	Upd(14)mat (n = 35)	Epimutation (n = 4)	Microdeletion (n = 4)
Premature delivery	−	−	−	−	−	10/25	0/4	0/3
Prenatal growth failure	−	+	+	+	+	24/27	4/4	3/3
Postnatal growth failure	+	+	+	+	+	26/32	3/4	3/3
Somatic features	+	+	+	+	+	23/35	4/4	3/3
Frontal bossing	+	+	+	+	−	9/9		
High arched palate	−	+	+		+	7/9		
Micrognathia	+	+	−	+	+	5/5		
Small hands	+	+	+	+	+	24/27	4/4	3/3
Scoliosis	−	−	−	−	−	5/19		
Others								
Hypotonia	+	+	+	+	+	25/28	4/4	1/1
Obesity	−	−	−	−	−	14/34	3/4	1/4
Early onset of puberty	NA	NA	NA	NA	NA	14/16	3/4	2/3
Mental retardation	−	−	−	−	+	10/27	2/4	1/4

NA, Not applicable.
Previous studies are based on references 2, 3 and 4.

Upd(14)mat syndrome demonstrates PWS-like phenotype during infancy, and it should be considered when seeing a patient with hypotonia. The *MEG3* methylation test should be performed to identify this syndrome. ■

The authors thank Dr. T. Ariga for critical reading of the manuscript.

Submitted for publication Mar 20, 2009; last revision received May 6, 2009; accepted Jun 22, 2009.

Reprint requests: Shinji Saitoh, MD, PhD, Department of Pediatrics, Hokkaido University, Graduate School of Medicine, North 15, West 7, Kita-ku, Sapporo, 060-8638, Japan. E-mail: ss11@med.hokudai.ac.jp.

References

1. Kotzot D, Utermann G. Uniparental disomy (UPD) other than 15: phenotypes and bibliography updated. Am J Med Genet A 2005;136: 287-305.
2. Kagami M, Sekita Y, Nishimura G, Irie M, Kato F, Okada M, et al. Deletions and epimutations affecting the human 14q32.2 imprinted region in individuals with paternal and maternal upd(14)-like phenotypes. Nat Genet 2008;40:237-42.
3. Hosoki K, Ogata T, Kagami M, Tanaka T, Saitoh S. Epimutation (hypomethylation) affecting the chromosome 14q32.2 imprinted region in a girl with upd(14)mat-like phenotype. Eur J Hum Genet 2008;16:1019-23.
4. Buiting K, Kanber D, Martín-Subero JI, Lieb W, Terhal P, Albrecht B, et al. Clinical features of maternal uniparental disomy 14 in patients with an epimutation and a deletion of the imprinted DLK1/GTL2 gene cluster. Hum Mutat 2008;29:1141-6.
5. Temple IK, Cockwell A, Hassold T, Pettay D, Jacobs P. Maternal uniparental disomy for chromosome 14. J Med Genet 1991;28:511-4.
6. Nicholls RD, Saitoh S, Horsthemke B. Imprinting in Prader-Willi and Angelman syndromes. Trends Genet 1998;14:194-200.
7. Mitter D, Buiting K, von Eggeling F, Kuechler A, Liehr T, Mau-Holzmann UA, et al. Is there a higher incidence of maternal uniparental disomy 14 [upd(14)mat]? Detection of 10 new patients by methylation-specific PCR. Am J Med Genet A 2006;140:2039-49.
8. Kubota T, Das S, Christian SL, Baylin SB, Herman JG, Ledbetter DH. Methylation-specific PCR simplifies imprinting analysis. Nat Genet 1997;16:16-7.
9. Murphy SK, Wylie AA, Coveler KJ, Cotter PD, Papenhausen PR, Sutton VR, et al. Epigenetic detection of human chromosome 14 uniparental disomy. Hum Mutat 2003;22:92-7.
10. Cox H, Bullman H, Temple IK. Maternal UPD(14) in the patient with a normal karyotype: clinical report and a systematic search for cases in samples sent for testing for Prader-Willi syndrome. Am J Med Genet A 2004;127A:21-5.
11. Temple IK, Shrubb V, Lever M, Bullman H, Mackay DJ. Isolated imprinting mutation of the DLK1/GTL2 locus associated with a clinical presentation of maternal uniparental disomy of chromosome 14. J Med Genet 2007;44:637-40.
12. Horsthemke B, Nazlican H, Hüsing J, Klein-Hitpass L, Claussen U, Michel S, et al. Somatic mosaicism for maternal uniparental disomy 15 in a girl with Prader-Willi syndrome: confirmation by cell cloning and identification of candidate downstream genes. Hum Mol Genet 2003;12:2723-32.

Table I. Microsatellite polymorphism analyses for chromosome 14 in 6 families with aberrant MRG9 methylation

Locus	Region	Case 1 family			Case 2 family			Case 3 family			Case 4 family			Case 5 family		
		Patient	Father	Mother	Patient	Father	Mother	Patient	Father	Mother	Patient	Father	Mother	Patient	Father	Mother
D14S261	14q11.2	298, 298	274, 298	298, 298	297, 297	297, 299	297, 297	298, 298	296, 298	298, 298	297, 297	297, 297	275, 297	275, 297, 297	275, 299	273, 297
D14S283	14q11.2	147, 149	139, 149	137, 147	139, 139	137, 137	139, 139	137, 149	133, 137	137, 149	150, 150	142, 150	140, 150	139, 139	137, 139	139, 147
D14S275	14q12	146, 146	146, 156	146, 146	149, 149	145, 145	149, 151	148, 152	146, 146	148, 152	155, 155	149, 155	149, 155	146, 148, 152	152, 156	146, 148
D14S70	14q13.1	100, 102	102, 102	100, 104	101, 101	101, 103	101, 101	103, 103	99, 101	103, 103	104, 104	104, 106	104, 104	101, 101, 103	101, 103	101, 101
D14S288	14q21.2	191, 201	201, 203	191, 207	201, 201	203, 203	201, 201	193, 193	193, 203	193, 193	195, 195	213, 215	195, 197	190, 196, 204	188, 196	190, 204
D14S276	14q22.3	241, —	239, 241	247, —	242, 244	244, 246	242, 244	244, 244	242, 244	244, 244	245, 245	241, 241	245, 245	244, 246, 246	242, 244	246, 246
D14S63	14q23.2	187, 187	187, 187	187, 187	187, 193	183, 189	187, 193	183, 187	189, 191	183, 187	191, 191	185, 195	191, 195	187, 189, 193	187, 193	187, 189
D14S258	14q24.2	204, 206	196, 206	202, 204	196, 196	198, 202	196, 196	196, 196	200, 202	196, 196	202, 202	204, 204	202, 204	196, 196, 198	198, 200	196, 196
D14S74	14q24.3	299, 313	260, 299	303, 313	303, 303	303, 305	303, 303	299, 303	299, 301	299, 303	295, 295	305, 313	295, 301	299, 301, 305	299, 305	299, 301
D14S68	14q31.3	323, 323	323, 323	323, 323	321, 321	323, 323	321, 321	321, 323	323, 323	321, 323	323, 323	325, 325	321, 323	321, 321, 323	323, 323	321, 321
D14S280	14q32.12	246, 248	248, 248	246, 246	243, 243	243, 245	243, 243	247, 247	243, 247	247, 247	248, 248	244, 244	242, 248	241, 243, 247	241, 245	243, 247
D14S65	14q32.2	135, 141	135, 135	135, 141	145, 145	135, 149	135, 145	135, 147	137, 145	135, 147	150, 150	150, 150	150, 150	135, 147	147, 147	135, 147
D14S985	14q32.2	255, 255	251, 255	255, 257	250, 250	246, 254	250, 254	247, 247	249, 249	247, 247	248, 248	246, 248	248, 254	247, 249	247, 253	247, 249
D14S292	14q32.33	84, 86	84, 86	86, 86	92, 92	86, 88	88, 92	85, 87	83, 85	85, 87	92, 92	86, 92	88, 92	87, 89	89, 89	87, 89

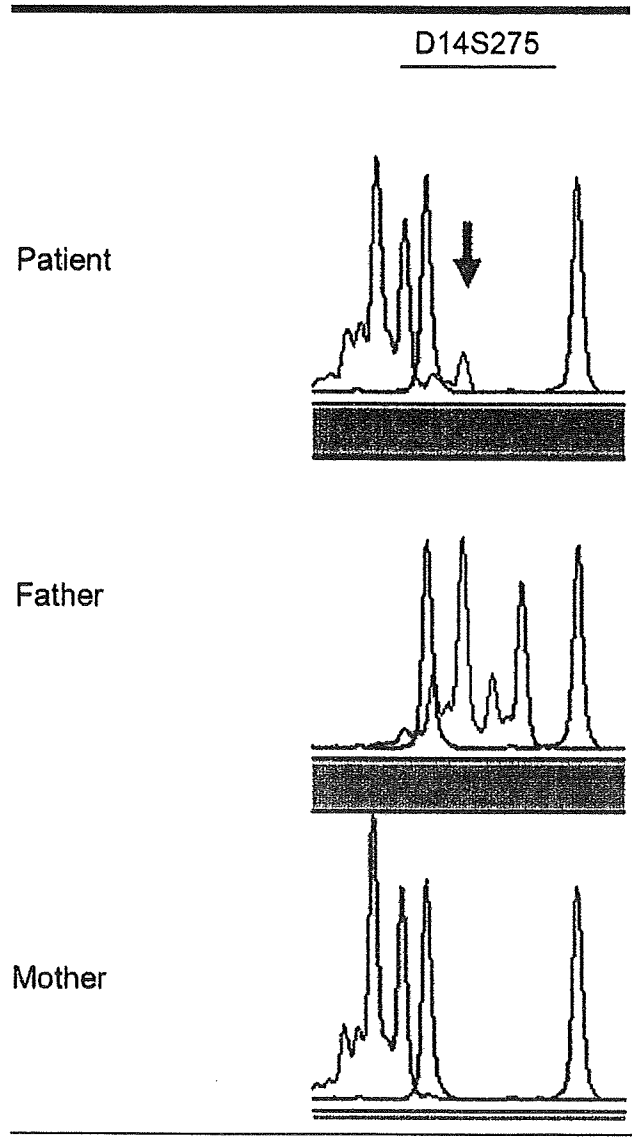

Figure 3. Microsatellite polymorphism analysis at D14S275 for the family of case 5. The patient demonstrates 3 peaks (146, 148, 152 bp), 2 (146, 148 bp) of which are transmitted from the mother, but 1 small peak (152 bp) indicated by the *arrow* is transmitted from the father. *Red peaks* depict size markers.

The IG-DMR and the *MEG3*-DMR at Human Chromosome 14q32.2: Hierarchical Interaction and Distinct Functional Properties as Imprinting Control Centers

Masayo Kagami[1], Maureen J O'Sullivan[2], Andrew J Green[3], Yoshiyuki Watabe[4], Osamu Arisaka[4], Nobuhide Masawa[5], Kentarou Matsuoka[6], Maki Fukami[1], Keiko Matsubara[1], Fumiko Kato[1], Anne C Ferguson-Smith[7], and Tsutomu Ogata[1]*

1 Department of Endocrinology and Metabolism, National Research Institute for Child Health and Development, Tokyo, Japan, **2** Department of Pathology, Our Lady's Children's Hospital, and School of Medicine, Trinity College, Dublin, Ireland, **3** National Center for Medical Genetics, University College Dublin, Our Lady's Hospital, and School of Medicine and Medical Science, University College, Dublin, Ireland, **4** Department of Pediatrics, Dokkyo University School of Medicine, Tochigi, Japan, **5** Department of Pathology, Dokkyo University School of Medicine, Tochigi, Japan, **6** Department of Pathology, National Center for Child Health and Development, Tokyo, Japan, **7** Department of Physiology, Development and Neuroscience, University of Cambridge, Cambridge, UK.

Running head: Imprinting Control Centers at Human 14q32.2

*Correspondence: tomogata@nch.go.jp.

Abstract

Human chromosome 14q32.2 harbors the germline-derived primary *DLK1-MEG3* intergenic differentially methylated region (IG-DMR) and the postfertilization-derived secondary *MEG3*-DMR, together with multiple imprinted genes. Although previous studies in cases with microdeletions and epimutations affecting both DMRs and paternal/maternal uniparental disomy 14 (upd(14)pat/mat)-like phenotypes argue for a critical regulatory function of the two DMRs for the 14q32.2 imprinted region, the precise role of individual DMR remains to be clarified. We studied an infant with upd(14)pat body and placental phenotypes (patient 1) and the mother with upd(14)mat-like body phenotype (patient 2), and a neonate with upd(14)pat body, but no placental, phenotype (patient 3). Structural analysis showed a familial 8,558 bp microdeletion involving the IG-DMR alone in patients 1 and 2, and a *de novo* 4,303 bp microdeletion involving the *MEG3*-DMR alone in patient 3. Methylation and expression analyses revealed that loss of the hypomethylated IG-DMR of maternal origin in patient 1 was associated with epimutation (hypermethylation) of the *MEG3*-DMR in the body and caused paternalization of the imprinted region in examined body and placental tissues, whereas loss of the hypomethylated *MEG3*-DMR of maternal origin in patient 3 permitted normal methylation pattern of the IG-DMR and resulted in maternal to paternal epigenotypic alteration in examined body tissues. The imprinting status appeared normal in patient 2. These results, together with the finding that the IG-DMR remains as a DMR and the *MEG3*-DMR exhibits a non-DMR in the placenta, imply that the IG-DMR and the *MEG3*-DMR function as imprinting control centers in the placenta and the body, respectively, with a hierarchical interaction for the methylation pattern in the body. In addition, the phenotype of patient 2 may suggest the presence of a *cis*-acting regulatory element for *DLK1* expression around the IG-DMR.

Author Summary

Human chromosome 14q32.2 imprinted region harbors the germline-derived primary *DLK1-MEG3* intergenic differentially methylated region (IG-DMR) and the postfertilization-derived secondary *MEG3*-DMR, together with multiple imprinted genes. Consistent with this, paternal and maternal uniparental disomy 14 (upd(14)pat and upd(14)mat) causes distinct phenotypes. Here, we show that the IG-DMR acts as an upstream regulator for the methylation pattern of the *MEG3*-DMR in the body but not in the placenta, and that the IG-DMR and the *MEG3*-DMR function as imprinting control centers in the placenta and the body, respectively. To our knowledge, this is the first study demonstrating not only different roles between the primary and the secondary DMRs at a single imprinted region, but also an essential regulatory function for the secondary DMR. Thus, the results provide significant advance in the clarification of underlying mechanisms involved in the imprinting regulation at the 14q32.2 region and the development of upd(14)pat/mat phenotype. In addition, we also suggest the presence of a *cis*-acting regulatory element for the *DLK1* expression around the IG-DMR.

Introduction

Human chromosome 14q32.2 carries a cluster of protein-coding paternally expressed genes (*PEGs*) such as *DLK1* and *RTL1* and non-coding maternally expressed genes (*MEGs*) such as *MEG3* (alias, *GTL2*), *RTL1as* (*RTL1* antisense), *MEG8*, *snoRNAs*, and *microRNAs* [1,2]. Consistent with this, paternal uniparental disomy 14 (upd(14)pat) results in a unique phenotype characterized by facial abnormality, small bell-shaped thorax, abdominal wall defects, placentomegaly, and polyhydramnios [2,3], and maternal uniparental disomy 14 (upd(14)mat) leads to less-characteristic but clinically discernible features including growth failure [2,4].

The 14q32.2 imprinted region also harbors two differentially methylated regions (DMRs), i.e., the germline-derived primary *DLK1-MEG3* intergenic DMR (IG-DMR) and the postfertilization-derived secondary *MEG3*-DMR [1,2]. Both DMRs are hypermethylated after paternal transmission and hypomethylated after maternal transmission in the body, whereas in the placenta the IG-DMR alone remains as a DMR and the *MEG3*-DMR is rather hypomethylated [1,2]. Furthermore, previous studies in cases with upd(14)pat/mat-like phenotypes have revealed that epimutations (hypermethylation) and microdeletions affecting both DMRs of maternal origin cause paternalization of the 14q32.2 imprinted region, and that epimutations (hypomethylation) affecting both DMRs of paternal origin cause maternalization of the 14q32.2 imprinted region, while microdeletions involving the DMRs of paternal origin have no effect on the imprinting status [2,5–8]. These findings, together with the notion that parent-of-origin specific expression patterns of imprinted genes are primarily dependent on the methylation status of the DMRs [9], argue for a critical regulatory function of the two DMRs for the 14q32.2 imprinted region, with possible different effects between the body and the placenta.

However, the precise role of individual DMR remains to be clarified. Here, we report that the IG-DMR and the *MEG3*-DMR show a hierarchical interaction for the methylation pattern in the body, and function as imprinting control centers in the placenta and the body, respectively. To our knowledge, this is the first study demonstrating not only different roles between the primary and secondary DMRs at a single imprinted region, but also an essential regulatory function for the secondary DMR.

Results

Clinical reports

We identified familial cases, a proband (patient 1) and the mother (patient 2), and a sporadic case (patient 3) Detailed phenotypes of patients 1 and 3 are summarized in Table 1 (see also Figure 1), and those of patient 2 are summarized in Table 2. In brief, patient 1 was delivered by a caesarean section at 33 weeks of gestation due to progressive polyhydramnios despite amnioreduction at 28 and 30 weeks of gestation, whereas patient 3 was born at 28 weeks of gestation by a vaginal delivery due to progressive labor without discernible polyhydramnios. Placentomegaly was observed in patient 1 but not in patient 3. Patients 1 and 3 were found to have characteristic face, small bell-shaped thorax with coat hanger appearance of the ribs, and omphalocele. Patient 1 received surgical treatment for omphalocele immediately after birth and mechanical ventilation for several months. At present, she is 5.5 months of age, and still requires intensive care including oxygen administration and tube feeding. Patient 3 died at four days of age due to massive intracranial hemorrhage, while receiving intensive care including mechanical ventilation. Thus, upd(14)pat body phenotype was unequivocally exhibited by patients 1 and 3, whereas upd(14)pat placental phenotype, which has invariably been identified by 28 weeks of gestation in upd(14)pat patients [2,3], was present in patient 1 and absent from patient 3. Patient 2 was noticed to have upd(14)mat-like body phenotype including short stature, obesity, and small hands, through familial studies. The father of patient 1 and the parents of patient 3 were clinically normal.

Sample preparation

We isolated genomic DNA (gDNA) and transcripts (*mRNAs*, *snoRNAs*, and *microRNAs*) from fresh leukocytes of patients 1 and 2, the father of patient 1, and the parents of patient 3, from fresh skin fibroblasts of patient 3, and from formalin-fixed and paraffin-embedded placental samples of patient 1 and similarly treated pituitary and adrenal samples of patient 3 (although multiple body tissues were available in patient 3, useful gDNA and transcript samples were not obtained from other tissues probably due to drastic post-mortem degradation). We also made metaphase spreads from leukocytes and skin fibroblasts. For comparison, we obtained

control samples from fresh normal adult leukocytes, neonatal skin fibroblasts, and placenta at 38 weeks of gestation, and from fresh leukocytes of upd(14)pat/mat patients and formalin-fixed and paraffin-embedded placenta of a upd(14)pat patient [2,3].

Structural analysis of the imprinted region

We first examined the structure of the 14q32.2 imprinted region (Figure 2). Upd(14) was excluded in patients 1–3 by microsatellite analysis (Table S1), and FISH analysis for the two DMRs identified a familial heterozygous deletion encompassing the IG-DMR alone in patients 1 and 2 and a *de novo* heterozygous deletion encompassing the *MEG3*-DMR alone in patient 3 (Figure 2). The microdeletions were further localized by SNP genotyping for 66 loci (Table S1) and quantitative real-time PCR (q-PCR) analysis for four regions around the DMRs (Figure S1A), and serial direct sequencing for the long PCR products harboring the deletion junctions successfully identified the fusion points of the microdeletions in patients 1–3 (Figure 2). According to the NT_026437 sequence data at the NCBI Database (Genome Build 36.3) (http://preview.ncbi.nlm.nih.gov/guide/), the deletion size was 8,558 bp (82,270,449–82,279,006 bp) for the microdeletion in patients 1 and 2, and 4,303 bp (82,290,978–82,295,280 bp) for the microdeletion in patient 3. The microdeletion in patient 3 also involved the 5' part of *MEG3* and five of the seven putative CTCF binding sites A–G [13], and was accompanied by insertion of a 66 bp sequence duplicated from *MEG3* intron 5 (82,299,727–82,299,792 bp on NT_026437). Direct sequencing of the exonic or transcribed regions detected no mutation in *DLK1*, *MEG3*, and *RTL1*, although several cDNA polymorphisms (cSNPs) were identified (Table S1). Oligoarray comparative genomic hybridization identified no other discernible structural abnormality (Figure S1B).

Methylation analysis of the two DMRs

We next studied methylation patterns of the previously reported IG-DMR (CG4 and CG6) and the *MEG3*-DMR (CG7) [2] and those of the seven putative CTCF binding sites, using bisulfite treated gDNA samples (Figure 3A). Bisulfite sequencing and combined bisulfite restriction analysis using body samples revealed a hypermethylated IG-DMR and *MEG3*-DMR

in patient 1, a hypomethylated IG-DMR and differentially methylated *MEG3*-DMR in patient 2, and a differentially methylated IG-DMR and hypermethylated *MEG3*-DMR in patient 3, and bisulfite sequencing using placental samples showed a hypermethylated IG-DMR and rather hypomethylated *MEG3*-DMR in patient 1 (Figure 3B). Furthermore, bisulfite sequencing revealed that, of the seven putative CTCF binding sites, sites C and D exhibited methylation patterns comparable to those of CG7 (Figure 3C).

Expression analysis of the imprinted genes

Finally, we performed expression analyses, using standard reverse transcriptase (RT)-PCR and/or q-PCR analysis for multiple imprinted genes in this region (Figure 4A–C). For leukocytes, weak expression was detected for *MEG3* and *SNORD114-29* in a control subject and patient 2 but not in patient 1. For skin fibroblasts, although all *MEGs* but no *PEGs* were expressed in control subjects, neither *MEGs* nor *PEGs* were expressed in patient 3. For placentas, although all imprinted genes were expressed in control subjects, *PEGs* only were expressed in patient 1. For the pituitary and adrenal of patient 3, *DLK1* expression alone was identified.

Expression pattern analyses using informative cSNPs revealed monoallelic *MEG3* expression in the leukocytes of patient 2 (Figure 4D), and biparental *RTL1* expression in the placenta of patient 1 (no informative cSNP was detected for *DLK1*) and biparental *DLK1* expression in the pituitary and adrenal of patient 3 (*RTL1* was not expressed in the pituitary and adrenal) (Figure 4E), as well as maternal *MEG3* expression in the control leukocytes and paternal *RTL1* expression in the control placentas (Figure S2). Although we also attempted q-PCR analysis, precise assessment was impossible for *MEG3* in patient 2 because of faint expression level in leukocytes and for *RTL1* in patient 1 and *DLK1* in patient 3 because of poor quality of mRNAs obtained from formalin-fixed and paraffin-embedded tissues.

Discussion

The data of the present study are summarized in Figure 5. Parental origin of the microdeletion positive chromosomes is based on the methylation patterns of the preserved

DMRs in patients 1–3 as well as maternal transmission in patient 1. Loss of the hypomethylated IG-DMR of maternal origin in patient 1 was associated with epimutation (hypermethylation) of the *MEG3*-DMR in the body and caused paternalization of the imprinted region and typical upd(14)pat body and placental phenotypes, whereas loss of the hypomethylated *MEG3*-DMR of maternal origin in patient 3 permitted normal methylation pattern of the IG-DMR in the body and resulted in maternal to paternal epigenotypic alteration and typical upd(14)pat body, but no placental, phenotype. In this regard, while a 66 bp segment was inserted in patient 3, this segment contains no known regulatory sequence [14] or evolutionarily conserved element [15] (also examined with a VISTA program, http://genome.lbl.gov/vista/index.shtml). Similarly, while no control samples were available for pituitary and adrenal, the previous study in human subjects has shown paternal *DLK1* expression in adrenal as well as monoallelic *DLK1* and *MEG3* expressions in various tissues [14]. Furthermore, the present and the previous studies [2] indicate that this region is imprinted in the placenta as well as in the body. Thus, these results, in conjunction with the finding that the IG-DMR remains as a DMR and the *MEG3*-DMR exhibits a non-DMR in the placenta [2], imply the following: (1) the IG-DMR functions hierarchically as an upstream regulator for the methylation pattern of the *MEG3*-DMR on the maternally inherited chromosome in the body, but not in the placenta; (2) the hypomethylated *MEG3*-DMR functions as an essential imprinting regulator for both *PEGs* and *MEGs* in the body; and (3) in the placenta, the hypomethylated IG-DMR directly controls the imprinting pattern of both *PEGs* and *MEGs*. These notions also explain the epigenotypic alteration in the previous cases with epimutations or microdeletions affecting both DMRs (Figure S3).

For the *MEG3*-DMR, the CTCF binding sites C and D may play a pivotal role in the imprinting regulation. The methylation analysis indicates that the two cites reside within the *MEG3*-DMR, and it is known that the CTCF protein with versatile functions preferentially binds to unmethylated target sequences including the sites C and D [13,16–18]. In this regard, all the *MEGs* in this imprinted region can be transcribed together in the same orientation and show a strikingly similar tissue expressions pattern [1,15], whereas *PEGs* are transcribed in different directions and are co-expressed with *MEGs* only in limited cell-types [1,19]. It is possible, therefore, that preferential CTCF binding to the grossly unmethylated sites C and D

activates all the *MEGs* as a large transcription unit and represses all the *PEGs* perhaps by influencing chromatin structure and histone modification independently of the effects of expressed *MEGs*. In support of this, CTCF protein acts as a transcriptional activator for *Gtl2* (the mouse homolog for *MEG3*) in the mouse [20].

Patient 2 had upd(14)mat-like body phenotype. This may be co-incidental, because her clinical features are not specific to upd(14)mat. Indeed, consistent with the notion that loss of the paternally derived IG-DMR does not affect the imprinted status [2,21], *MEG3* showed normal monoallelic expression in the presence of the differentially methylated *MEG3*-DMR. However, since upd(14)mat phenotype is primarily ascribed to loss of functional *DLK1* with an additional effect of loss of functional *RTL1* (Figure S3B) [2,22,23], the microdeletion involving the IG-DMR may have affected a *cis*-acting regulatory element for *DLK1* expression (Figure 5). In this case, the microdeletion is predicted to affect *DLK1* expression on the paternalized chromosome of maternal origin in patient 1. However, this is not inconsistent with the typical upd(14)pat phenotype in patient 1, because patient 1 had clear biparental *RTL1* expression in the absence of *MEGs* expression. Indeed, typical upd(14)pat body and placental phenotype has primarily been ascribed to markedly elevated *RTL1* expression, which is explained by the synergic effect of two active copies of *RTL1* and the absence of functional *RTL1as* as a repressor for *RTL1* [21,23–25], rather than to doubled *DLK1* expression (Figure S3A) [2].

This imprinted region has also been studied in the mouse. Clinical and molecular findings in wildtype mice [1,26,27], mice with PatDi(12) (paternal disomy for chromosome 12 harboring this imprinted region) [28–30], and mice with targeted deletions for the IG-DMR (ΔIG-DMR) [21,26] and for the *Gtl2*-DMR (the mouse homolog for the *MEG3*-DMR) (Δ*Gtl2*-DMR) [31] are summarized in Table 3. These data, together with human data, provide several informative findings. First, in both the human and the mouse, the IG-DMR is differentially methylated in both the body and the placenta, whereas the *MEG3/Gtl2*-DMR is differentially methylated in the body and exhibits non-DMR in the placenta. Second, the IG-DMR and the *MEG3/Gtl2*-DMR show a hierarchical interaction on the maternally derived chromosome in both the human and the mouse bodies. Indeed, the *MEG3/Gtl2*-DMR is epimutated in patient 1 and mice with maternally inherited ΔIG-DMR, and the IG-DMR is

normally methylated in patient 3 and mice with maternally inherited Δ*Gtl2*-DMR. Third, the function of the IG-DMR is comparable between human and mouse bodies and different between human and mouse placentas. Indeed, patient 1 has upd(14)pat body and placental phenotypes, whereas mice with the ΔIG-DMR of maternal origin have PatDi(12)-compatible body phenotype and apparently normal placental phenotype. It is likely that imprinting regulation in the mouse placenta is contributed by some mechanism(s) other than the methylation pattern of the IG-DMR, such as chromatin conformation [26,32,33].

Unfortunately, however, the data of Δ*Gtl2*-DMR mice appears to be drastically complicated by the retained neomycin cassette in the upstream region of *Gtl2*. Indeed, it has been shown that the insertion of a *lacZ* gene or a neomycin gene in the similar upstream region of *Gtl2* causes severely dysregulated expression patterns and abnormal phenotypes after both paternal and maternal transmissions [34,35], and that deletion of the inserted neomycin gene results in apparently normal expression patterns and phenotypes after both paternal and maternal transmissions [35]. (In this regard, although a possible influence of the inserted 66 bp segment can not be excluded formally in patient 3, phenotype and expression data in patient 3 are compatible with simple paternalization of the imprinted region.) In addition, since the apparently normal phenotype in mice homozygous for Δ*Gtl2*-DMR is reminiscent of that in sheep homozygous for the callipyge mutation [36], a complicated mechanism(s) such as the polar overdominance may be operating in the Δ*Gtl2*-DMR mice [37]. Thus, it remains to be clarified whether the *MEG3/Gtl2*-DMR has a similar or different function between the human and the mouse.

In summary, the results show a hierarchical interaction and distinct functional properties of the IG-DMR and the *MEG3*-DMR in imprinting control. Thus, this study provides significant advance in the clarification of underlying mechanisms involved in the imprinting regulation at the 14q32.2 imprinted region and the development of upd(14)pat/mat phenotype.

Methods

Ethics Statement

This study was approved by the Institutional Review Board Committees at National Center for Child health and Development, University College Dublin, and Dokkyo University School of Medicine, and performed after obtaining written informed consent.

Primers

All the primers utilized in this study are summarized in Table S2.

Sample preparation

For leukocytes and skin fibroblasts, genomic DNA (gDNA) samples were extracted with FlexiGene DNA Kit (Qiagen), and RNA samples were prepared with RNeasy Plus Mini (Qiagen) for *DLK1, MEG3, RTL1*, *MEG8* and *snoRNAs*, and with mirVana™ miRNA Isolation Kit (Ambion) for *microRNAs*. For paraffin-embedded tissues including the placenta, brain, lung, heart, liver, spleen, kidney, bladder, and small intestine, gDNA and RNA samples were extracted with RecoverAll™ Total Nucleic Acids Isolation Kit (Ambion) using slices of 40 μm thick. For fresh control placental samples, gDNA and RNA were extracted using ISOGEN (Nippon Gene). After treating total RNA samples with DNase, cDNA samples for *DLK1, MEG3, MEG8*, and *snoRNAs* were prepared with oligo(dT) primers from 1 μg of RNA using Superscript III Reverse Transcriptase (Invitrogen), and those for *microRNAs* were synthesized from 300 ng of RNA using TaqMan MicroRNA Reverse Transcription Kit (Applied Biosystems). For *RTL1*, cDNA samples were synthesized with *RTL1*-specific primers that do not amplify *RTL1as*. Control gDNA and cDNA samples were extracted from adult leukocytes and neonatal skin fibroblasts purchased from Takara Bio Inc. Japan, and from a fresh placenta of 38 weeks of gestation. Metaphase spreads were prepared from leukocytes and skin fibroblasts using colcemide (Invitrogen).

Structural analysis

Microsatellite analysis and SNP genotyping were performed as described previously [2].

For FISH analysis, metaphase spreads were hybridized with a 5,104 bp FISH-1 probe and a 5,182 bp FISH-2 probe produced by long PCR, together with an RP11-566I2 probe for 14q12 used as an internal control [2]. The FISH-1 and FISH-2 probes were labeled with digoxigenin and detected by rhodamine anti-digoxigenin, and the RP11-566I2 probe was labeled with biotin and detected by avidin conjugated to fluorescein isothiocyanate. For quantitative real-time PCR analysis, the relative copy number to RNaseP (catalog No: 4316831, Applied Biosystems) was determined by the Taqman real-time PCR method using the probe-primer mix on an ABI PRISM 7000 (Applied Biosystems). To determine the breakpoints of microdeletions, sequence analysis was performed for long PCR products harboring the fusion points, using serial forward primers on the CEQ 8000 autosequencer (Beckman Coulter). Direct sequencing was also performed on the CEQ 8000 autosequencer. Oligoarray comparative genomic hybridization was performed with 1x244K Human Genome Array (catalog No: G4411B) (Agilent Technologies), according to the manufacturer's protocol.

Methylation analysis

Methylation analysis was performed for gDNA treated with bisulfite using the EZ DNA Methylation Kit (Zymo Research). After PCR amplification using primer sets that hybridize both methylated and unmethylated clones because of lack of CpG dinucleotides within the primer sequences, the PCR products were digested with appropriate restriction enzymes for combined bisulfite restriction analysis. For bisulfite sequencing, the PCR products were subcloned with TOPO TA Cloning Kit (Invitrogen) and subjected to direct sequencing on the CEQ 8000 autosequencer.

Expression analysis

Standard RT-PCR was performed for *DLK1*, *RTL1*, *MEG3*, *MEG8*, and *snoRNAs* using primers hybridizing to exonic or transcribed sequences, and one μl of PCR reaction solutions was loaded onto Gel-Dye Mix (Agilent). Taqman real-time PCR was carried out using the probe-primer mixtures (assay No: Hs00292028 for *MEG3* and Hs00419701 for *MEG8*; assay ID: 001028 for *miR433*, 000452 for *miR127*, 000568 for *miR379*, and 000477 for *miR154*) on